PHYSICAL REVIEW B **77**, 064303 (2008)

Raman scattering in KOs_2O_6

Takumi Hasegawa,* Yuichi Takasu, Norio Ogita, and Masayuki Udagawa
Graduate School of Integrated Arts and Sciences, Hiroshima University, 1-7-1 Kagamiyama, Higashi-Hiroshima, Hiroshima 739-8521, Japan

Jun-Ichi Yamaura, Yohei Nagao, and Zenji Hiroi
Institute for Solid State Physics, The University of Tokyo, 5-1-5 Kashiwanoha, Kashiwa, Chiba 277-8581, Japan

(Received 8 October 2007; revised manuscript received 4 December 2007; published 26 February 2008)

KOs_2O_6 with a β-pyrochlore structure undergoes a superconducting transition at T_c=9.6 K, which is the highest temperature among a series of compounds, AOs_2O_6 (A=K, Rb, and Cs). In this structure, it is expected that vibrations of the atoms have a large amplitude and a large anharmonicity because an alkali atom is weakly bounded in a large space. On the other hand, KOs_2O_6 shows another transition at T_p=7.5 K, which is considered as a structural transition. Moreover, two structures have been reported at room temperature. To investigate structures and anharmonicity of vibrations, Raman scattering spectra of KOs_2O_6 have been measured from 4 K to room temperature. Six Raman-active modes are successfully assigned. The assignment concludes that the symmetry at room temperature is $Fd\bar{3}m$, not $F\bar{4}3m$. A vibration of potassium at 70 cm^{-1} with a T_{2g} symmetry clearly shows a large anharmonicity. Moreover, a similar large anharmonicity has also been observed for the oxygen cage modes with the symmetries of E_g at 260 cm^{-1} and T_{2g} at 240 cm^{-1}. The electron-lattice interaction is estimated by the linewidth. The strongest interaction is that of the T_{2g} mode at 710 cm^{-1}, which modifies the bond length between osmium and oxygen, and the next one is E_g. The lack of phonon anomaly at T_c and T_p suggests that the E_u mode seems to be important for T_c and T_p since this E_u mode has the low-energy and strong electron-lattice interactions, judging from the similar displacement with the E_g mode.

DOI: 10.1103/PhysRevB.77.064303 PACS number(s): 63.20.−e, 78.30.−j

I. INTRODUCTION

Recently, a large amplitude oscillation of atoms, weakly bounded in large cages, has attracted much attention because of not only the application of thermoelectricity but also its possibility to provide interesting phenomena, for example, enhancement superconducting temperature[1–3] and occurrence of heavy-fermionic behavior.[4] β-pyrochlore of AOs_2O_6 (A=K, Rb, and Cs) has the large cage space constructed by oxygen. A ion in the β-pyrochlore is weakly bounded in a large cage space since the $A_2'O'$ unit in the α-pyrochlore $A_2'B_2O_6O'$ is replaced by the A ion in the β-pyrochlore. In fact, the large atomic displacement of the A ion have been observed in β-pyrochlore,[5,6] and its very low-energy vibration contributes to the anomalous lattice specific heat[2,7,8] and to the anomalous relaxation time of potassium in NMR.[9]

In general, vibrations of atoms weakly bounded in a large cage space have effectively large anharmonic potentials, compared with their relatively small harmonic potentials. In this case, their energies are greatly influenced by anharmonic potentials. As a result, the temperature dependence of their energy becomes quite different from normal lattice vibrations, where the energy of phonon increases with decreasing temperature due to thermal expansion effect. However, for a phonon affected by the large anharmonic potentials, its energy decreases mainly due to the fourth-order potentials. Many observations of this anharmonic effect have been recently reported for many cage structure compounds with a large cage size compared to the small ionic radii of the guest atom.[10–13] From these observations, it is concluded that the effect of anharmonicity becomes large for a larger cage and a smaller guest atom, and its energy becomes low. In KOs_2O_6, there is a large cage space where potassium moves easily, and the large atomic displacement parameter of potassium has been reported.[5,6] Therefore, the large anharmonic effect for energies of the K vibrations is expected.

Furthermore, β-pyrochlore structure oxides of AOs_2O_6 (A=K, Rb, and Cs) show superconductivity below 9.6, 6.3, and 3.3 K, respectively.[14–17] An α-pyrochlore structure, $Cd_2Re_2O_7$, also undergoes superconducting transition at 1.0 K,[18–20] but this transition temperature is lower than that of the β-pyrochlore compounds. Especially, KOs_2O_6 with the smallest alkali ionic radii exhibits strong-coupling superconductivity in contrast to other three α- and β-pyrochlore superconductors.[2] These facts suggest that the large amplitude and high anharmonicity of the potassium vibration relate to the relatively high T_c. Discussions about the mechanisms of superconductivity have been reported in this viewpoint for KOs_2O_6.[1,21–23]

KOs_2O_6 has another transition at T_p=7.5 K,[2,8,24] where specific heat shows a clear peak. Since this transition temperature is almost independent of magnetic field, it is considered as a structural transition. However, its details remain unclear. On the other hand, even for the structure of KOs_2O_6 at room temperature, there are two structural suggestions with space groups of $Fd\bar{3}m$ (Ref. 5) and $F\bar{4}3m$ (Ref. 6) by x-ray diffraction measurements. Then, another method is necessary to determine the structure at room temperature. Raman scattering experiments are very sensitive to structural deformations and, especially, are useful in distinguishing the similar structures with the different symmetry.

II. EXPERIMENTAL PROCEDURE

Single crystals of KOs_2O_6 were synthesized, as reported previously.[5,14] Raman scattering spectra were analyzed by a triple monochromator (JASCO NR-1800) and detected by a liquid-N_2 cooled charge coupled device (CCD) detector (Princeton Instruments Inc. LN/CCD-1100PB). For excitation light, a 514.5 nm line of an Ar^+ laser (Modu-Laser STELLAR-PRO-L) was employed and the natural emission lines were excluded by a premonochromator. A power of the incident light was 10 mW before a sample surface. For the measurements at low temperatures, a cryostat cooled by a GM cryocooler (SHI SRDK-205) was used. The energy of measured spectra was corrected using natural emission lines of a He-Ne laser. An error of absolute energy was about 1.5 cm^{-1} in this correction method, and an error of relative energy in a spectrum was about 0.7 cm^{-1}.

Raman spectra were measured on as-grown surfaces. The crystal axes were determined from polarization dependences of Raman spectra. Polarization directions of the incident and scattered light are described as (y,z), where y and z vectors in the parentheses are the directions of electric field of incident and scattered light, respectively. Propagation directions of incident and scattered light are omitted because the backscattering configuration was used.

III. SYMMETRY OF RAMAN-ACTIVE MODE

Two structures with the space group $Fd\bar{3}m$ (Ref. 5) or $F\bar{4}3m$ (Ref. 6) have been reported at room temperature. The difference between the two structures is a size of empty regular octahedra which are surrounded by four OsO_6 octahedra. There are two empty octahedra in the primitive unit cells for both structures. Both empty octahedra have the same size in the $Fd\bar{3}m$ structure, while their size is different in the $F\bar{4}3m$ structure. The $F\bar{4}3m$ structure is slightly distorted from the $Fd\bar{3}m$ structure and has no inversion symmetry. As a result, the $F\bar{4}3m$ structure has more Raman-active phonons than the $Fd\bar{3}m$ structure. Therefore, the number of the observed Raman-active phonons determines which structure is correct at room temperature.

In both structures, the primitive unit cell consists of 2 KOs_2O_6 f.u., i.e., 18 atoms. The irreducible representations of phonons at the Brillouin zone center are given for $Fd\bar{3}m$ as

$$\Gamma = \underline{A_{1g}} \oplus 2A_{2u} \oplus \underline{E_g} \oplus 2E_u \oplus 2T_{1g} \oplus 6T_{1u} \oplus 4\underline{T_{2g}} \oplus 3T_{2u} \tag{1}$$

and for $F\bar{4}3m$ as

$$\Gamma = 3\underline{A_1} \oplus 3\underline{E} \oplus 5T_1 \oplus 10\underline{T_2}, \tag{2}$$

where the underlined irreducible representations denote Raman-active phonons. The representations of the Raman-active optical phonon are $A_{1g} \oplus E_g \oplus 4T_{2g}$ and $3A_1 \oplus 3E \oplus 9T_2$ for the $Fd\bar{3}m$ and $F\bar{4}3m$ structures, respectively. The representation of a soft mode, which relates to a structural change from the $Fd\bar{3}m$ structure to the $F\bar{4}3m$ structure, is A_{2u} in the space group $Fd\bar{3}m$. Therefore, if the structure at room temperature is the $F\bar{4}3m$, the soft mode can be observed at the low-energy region as the A_1 representation of the space group $F\bar{4}3m$.

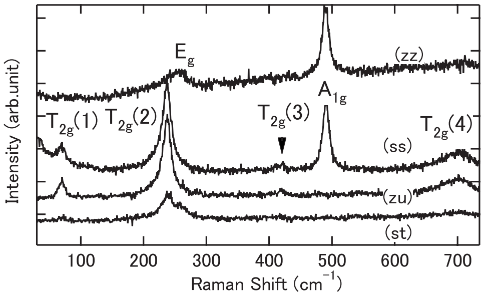

FIG. 1. Raman spectra of KOs_2O_6 at room temperature and a representation of each peak. The spectra were measured on the (110) surface. The vectors z, u, s, and t are (0, 0, 1), (1, −1, 0), (0.5, −0.5, 0.71), and (0.5, −0.5, −0.71), respectively.

In the $Fd\bar{3}m$ structure, since all Os atoms locate at inversion centers, all Raman-active phonons are the vibrations of potassium and oxygen. The vibrational freedoms of potassium are decomposed to two representations $T_{1u} \oplus T_{2g}$, and the T_{2g} mode appears in Raman spectra. The other modes, $A_{1g} \oplus E_g \oplus 3T_{2g}$, are vibrations of oxygen. On the other hand, in the $F\bar{4}3m$ structure, osmium vibrations become Raman active. The representations of the K vibrations are $2T_2$, which are Raman active. Since potassium ions are very weakly bounded in a large space built by OsO_6 octahedra, vibrations of potassium ions are expected to appear at a low-energy region. In the $F\bar{4}3m$ structure, two potassium $2T_2$ modes should be observed in addition to the soft A_1 mode in the low-energy region, but only one T_{2g} mode for the $Fd\bar{3}m$ structure.

IV. RESULTS AND DISCUSSION

In order to confirm the influence of impurity, the measurements at room temperature were performed on a number of surfaces of different samples and at several positions of the same surface since as-grown surfaces were used. Although some peaks from impurities due to OsO_2 and KO_2 were found at few positions, most of the measured positions showed the same spectra with six peaks. The crystal axes were determined by the sample rotation dependence of the intensity of T_{2g} or T_2 modes. In Fig. 1, the observed spectra on a (1 1 0) surface are shown, together with irreducible representations of $Fd\bar{3}m$, since the structure at room temperature is determined as $Fd\bar{3}m$, as described below. The peak assignment was made by the precise polarization dependence at room temperature. The polarization vectors in the figure denote $s=(0.5,-0.5,0.71)$, $t=(0.5,-0.5,-0.71)$, $u=(1,-1,0)$, and $z=(0,0,1)$. As seen in the results, the observed phonons are completely consistent with the $Fd\bar{3}m$ structure; i.e., the representations of the observed six peaks are $A_{1g} \oplus E_g \oplus 4T_{2g}$. The A_1 soft mode, which is expected in the $F\bar{4}3m$ structure, was not observed above 25 cm^{-1}. Therefore, the structure at room temperature is suggested as $Fd\bar{3}m$.

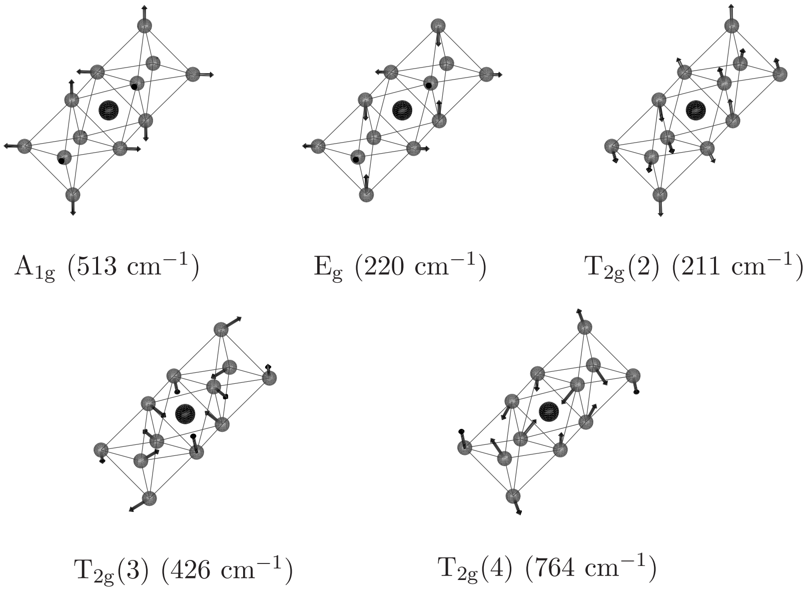

A_{1g} (513 cm^{-1}) E_g (220 cm^{-1}) $T_{2g}(2)$ (211 cm^{-1})

$T_{2g}(3)$ (426 cm^{-1}) $T_{2g}(4)$ (764 cm^{-1})

FIG. 2. Atomic displacements of five Raman-active oxygen modes. The black or gray circles denote Os or oxygen, respectively. The pictures show only three octahedra in the crystal structure, i.e., an OsO_6 octahedron and two regular octahedra beside the OsO_6. This part includes all oxygen atoms in the primitive cell. Oxygen atoms move to and/or away from potassium atoms in the A_{1g} and E_g modes. The calculated energies are also shown in parentheses.

This conclusion is also supported by the recent detailed structure analysis by x-ray and electron diffraction measurements.[25] Four T_{2g} modes are labeled as $T_{2g}(1)$, $T_{2g}(2)$, $T_{2g}(3)$, and $T_{2g}(4)$ from the lower energy. The lowest energy $T_{2g}(1)$ mode is the K vibration, and the other modes are the vibrations due to oxygen.

The observed phonon number and irreducible representations are well explained by the $Fd\bar{3}m$ structure. However, in order to exclude the possibility of $F\bar{4}3m$ completely, the discussion from other points of view is necessary. In $Cd_2Re_2O_7$ with the same symmetry of $Fd\bar{3}m$ at room temperature, an additional oxygen at the $8b$ site gives an extra oxygen T_{2g} mode instead of the potassium $T_{2g}(1)$ mode; however, the extra oxygen mode has not been observed.[26,27] Other phonon modes of $A_{1g} \oplus E_g \oplus 3T_{2g}$ are quite similar at room temperature. Furthermore, $Cd_2Re_2O_7$ undergoes structural transitions at 200 and 120 K, where the Raman spectra have changed dramatically.[26] Thus, the similar change should be found if the symmetry is lower than that of $Fd\bar{3}m$. In addition, a very recent inelastic neutron scattering experiment at room temperature[28] has reported the peak of phonon density of states at 6.4 meV due to the potassium modes, which corresponds to the Raman inactive T_{1u} mode for $Fd\bar{3}m$ but active for $F\bar{4}3m$. Thus, the extra mode at $\sim$50 cm^{-1} should be observed, but no peak at around 50 cm^{-1}. Therefore, the above discussion concludes that the structure at room temperature is $Fd\bar{3}m$.

Atomic displacements of five oxygen Raman-active phonons are shown in Fig. 2, where two empty octahedra and one OsO_6 octahedron are illustrated, and black or gray circles denote Os or oxygen, respectively. They have been obtained by first-principles calculation using the ABINIT package.[29,30] The calculated energies are also shown for the five oxygen vibrations. The detailed calculation methods and calculated energies of other important modes are described at the end of this section. The empty octahedron is found at the center of the tetrahedron made by four osmium atoms. In the primitive cell, there are two empty octahedra constructed by oxygen, which are also transformed each other by the inversion symmetry. Thus, there are two vibrational modes with a similar displacement: inversion symmetric Raman-active modes (A_{1g}, E_g, and T_{2g}) and asymmetric modes (A_{2u}, E_u, and T_{1u}) with the opposite direction displacements in two empty octahedrons.

For the low temperature measurements, the employed surface was (1 1 1), where all Raman-active phonons appear in a parallel polarization geometry. The representative Raman spectra at 4, 8, and 12 K are shown in Fig. 3, where two transitions at T_c=9.6 K and T_p=7.5 K are sandwiched. Unfortunately, in the present accuracy, no obvious change at these transition temperatures has been observed above 25 cm^{-1} in spite of the tiny intensity change observed by the x-ray diffraction peak at T_p.[25] Thus, more fine measurements with a higher resolution are necessary to detect the very small change of Raman spectra below 25 cm^{-1} at T_p or T_c.

Temperature variations on energies of five phonons without $T_{2g}(3)$, which has a very weak intensity, are shown in Fig. 4. The energies of $T_{2g}(1)$, $T_{2g}(2)$, and E_g decrease linearly from room temperature to low temperatures. This

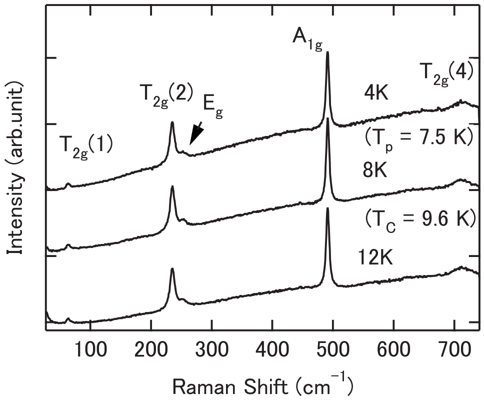

FIG. 3. Raman spectra of KOs_2O_6 at 4, 8, and 12 K. Two transition temperatures, T_c and T_p, are also shown.

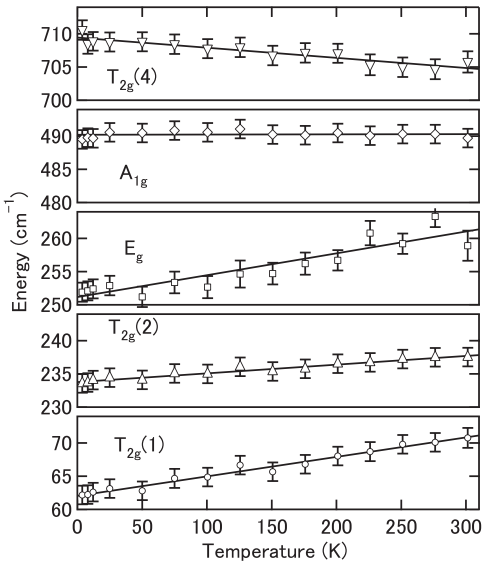

FIG. 4. Temperature dependence of observed phonon energy. The lines are least-squares fitting results using a linear function.

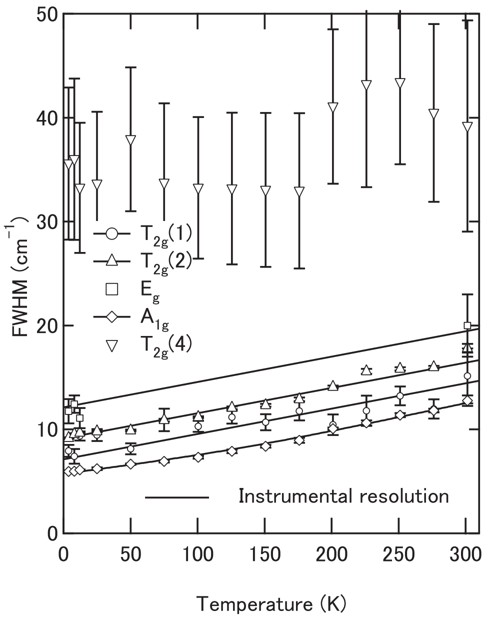

FIG. 5. Temperature dependence of the FWHM.

anomalous temperature dependence has also been observed in clathrate compounds[10,11] and skutterudites.[13] This anomaly is well explained by the large fourth-order anharmonic contribution for the weakly bounded guest ion in a large cage space.[10] In the above cases, the anomaly has been found only for the vibration of the guest ion. Thus, the present result is quite different from the previous report because the anomaly has been found not only for the $T_{2g}(1)$ mode of potassium, but also for two low-energy cage-oxygen modes of $T_{2g}(2)$ and E_g. Energy differences between room temperature and 4 K are obtained as 8.9, 4.0, and 7.0 cm^{-1} for $T_{2g}(1)$, $T_{2g}(2)$, and E_g, respectively. It is worthy to note that the difference for E_g is quite large. This suggests that vibrations of oxygen itself are highly anharmonic.

If we treat anharmonic interactions as a perturbation from harmonic oscillators, the energy of phonon, $\omega(T)$, is written as $\omega(T)^2=\omega_0^2+\Delta(T)$, where ω_0 is the energy of a harmonic oscillator and $\Delta(T)$ is a self-energy generated by the anharmonic interactions. The observed energy difference is given by $\omega(300\text{ K})-\omega(4\text{ K})=\{\Delta(300\text{ K})-\Delta(4\text{ K})\}/2\omega_0$. Since the three modes with large energy differences largely modulate the nearest K-O bond length, anharmonic interactions between potassium and oxygen are important. The x-ray diffraction measurement[5] has shown that the atomic displacement parameter $\langle u^2\rangle$ of potassium is very large. Therefore, the consideration of only anharmonic contribution due to potassium vibrations is an acceptable assumption. However, under this assumption, $T_{2g}(2)$ and E_g have smaller self-energies than $T_{2g}(1)$. Even under the assumption of the same self-energy for these three modes, the change in energy for $T_{2g}(2)$ and E_g is at most 3 cm^{-1} between room temperature and 4 K.

Especially for the E_g mode with large anharmonicity, it is impossible to explain the large change in energy using only large $\langle u^2\rangle$ of potassium since the estimated energy difference is much smaller than the measured value of 7 cm^{-1}. This discrepancy clearly shows that the vibrations of oxygen also have a large amplitude and are highly anharmonic. On the other hand, the observed atomic displacement parameter of oxygen is one-sixth of that of potassium.[5,6] Thus, the simple assumption, that the large anharmonic effect appears for the vibration with the large atomic displacement parameter, collapses in this system. In the oxygen mode case, a very small amount of the vibrational freedoms of oxygen constructs the low-energy mode. These oxygen vibrations remarkably contrast with the potassium case since the energy of all vibrations of potassium is low. Thus, it is necessary to consider the extra origin due to the similar low-energy phonons through the anharmonic interactions for the oxygen case. As the counterphonon, we consider the oxygen E_u mode, which has the opposite displacement to E_g. It is not strange that the E_u mode has low energy in KOs_2O_6 since the E_u mode plays as the soft mode for the structural phase transition at 200 K in $Cd_2Re_2O_7$.[27,31–33]

Next, we show the full width at half maximum (FWHM) of the observed peaks at various temperatures in Fig. 5. The data for $T_{2g}(3)$ are not shown because of its too small intensity. Unfortunately, the widths of E_g have not been accurately determined at high temperatures, where the E_g mode appears as the side peak of the $T_{2g}(2)$ mode. Thus, the data only below 20 K and at room temperature are shown for E_g. Below 20 K, the E_g and $T_{2g}(2)$ modes are observed as two peaks, as shown in Fig. 3. On the other hand, at room temperature, the E_g mode was observed separately in the (zz) spectra on the (110) surface, as shown in Fig. 1. Regarding $T_{2g}(4)$, it is difficult to determine the width because this mode has a very large width and a weak intensity and also because the maximum of the broad background structure located near its peak energy. By these difficulties, the widths of the $T_{2g}(4)$ mode depend largely on a background structure. An estimation of this error is at least 5 cm^{-1}. Results using the linear function for the background structure are shown and the error of the widths of the $T_{2g}(4)$ mode includes the error caused by the background structure, about 5 cm^{-1}.

The widths of A_{1g}, E_g, $T_{2g}(1)$, and $T_{2g}(2)$ modes linearly decrease down to at least 10 K. This temperature dependence is dominated by the scattering due to low-energy excitations of both phonons and electron. At high temperature region, the contribution of phonons increases owing to the increase of the number of thermally excited phonons, while a number of the thermally excited phonons vanish and the contribution of electron becomes dominant at low temperatures. The electron part is considered as temperature independent under the condition of no structural change.[34] The same gradients for these four modes show that the scattering by phonons is similar and the value at 4 K is recognized as the electronic contribution. Thus, the difference of the widths at 4 K corresponds to the difference of the magnitude of the electron-lattice interactions; that is, the E_g mode has the largest electron-lattice interactions among these modes. On the other hand, the width of $T_{2g}(4)$ is almost temperature independent in spite of the large data scattering. Although a discontinuous change is seen between 175 and 200 K, we cannot point it out within the present large error for the width of $T_{2g}(4)$. This result indicates that the lifetime of $T_{2g}(4)$ is determined mainly by the very strong electron-lattice interaction. Among five modes shown here, the mode affected by the strongest electron-lattice interaction is $T_{2g}(4)$, and the next one is E_g.

$T_{2g}(4)$ significantly modifies the bond lengths between osmium and oxygen and has large electron-lattice interactions because electronic states near Fermi surfaces are constructed by d electrons of osmium and p electrons of oxygen.[2,35,36] However, since the corresponding mode of $Cd_2Re_2O_7$ with low T_c has a similar linewidth, $T_{2g}(4)$ cannot be considered as the origin of superconductivity. As described above, the E_g mode also has strong electron-lattice interactions. This suggests the possibility that the opposite oxygen mode of E_u has intensive electron-lattice interactions. Thus, the E_u mode will be related to the superconductivity in KOs_2O_6.

Finally, the calculation methods and calculated energies of important modes are described. The first-principles calculation is performed with the ABINIT package.[29,30] It is based on first-principles pseudopotentials and a plane-wave basis set in the framework of the density-functional theory.[37] The local density approximation[38] is adopted for exchange-correlation energy, and the energy presented by Perdew and Wang[39] is used. The Troullier-Martins-type[40] pseudopotentials are generated using the FHI98PP code.[41] The K pseudopotential includes inner s and p states in addition to outer states. In the present calculation, a non-spin-polarized state is assumed, and spin-orbit interactions are not included. Calculations of phonon energies at the Γ point are performed within the density-functional perturbation theory.[42,43] Cutoff energies of the plane-wave basis set are 68 Ry, where 1 Ry $=13.606$ eV. For the integration of the Brillouin zone, special points[44] on Monkhorst-Pack $4\times4\times4$ k-point grids are used with the smearing energy of 0.02 Ry. The structure is relaxed within the space group $Fd\bar{3}m$, and then phonon energies are calculated with the structures. The determined lattice constant a is 10.172 Å, and the obtained position is (0.19165 0 0) for oxygen against (0.125 0.125 0.125) for Os. With the parameters for the integration in the Brillouin zone, we did not confirm conservation of phonon energies. The calculation error of phonon energies is estimated as at least 40 cm^{-1} for modes below 200 cm^{-1} by examining calculations with several parameters. In this paper, we use the calculated result for the displacement of the Raman-active oxygen modes. Since the displacement of the Raman-active modes is not sensitive to the parameters, the displacements, shown in Fig. 2, can be safely employed.

The important modes for KOs_2O_6 are A_{2u}, E_u, and potassium vibrations T_{1u} and T_{2g}, in addition to the Raman-active modes. The calculated energies for these modes are 291 and 453 cm^{-1} for two A_{2u} modes, $i286$ cm^{-1} for the E_u mode, and $i237$ and 48 cm^{-1} for potassium T_{1u} and T_{2g} modes, respectively. The imaginary frequencies mean that the modes are unstable soft modes. Therefore, the calculated result qualitatively agrees with the present conclusions; i.e., A_{2u} modes are not soft and the $F\bar{4}3m$ structure is not stable, and the E_u mode has a very low energy. The calculated result indicates that the soft E_u mode drives the structural transition to the $I\bar{4}m2$ symmetry. However, the energy difference between the calculated and experimental results is relatively large. This is probably due to the noninclusion of spin-orbit interactions and/or coarse k-point grids. Therefore, we do not discuss the calculated energies and stable structures using the present calculation results.

V. CONCLUSIONS

Raman spectra of KOs_2O_6 were measured from 4 K to room temperature. Although two structures with space groups $Fd\bar{3}m$ and $F\bar{4}3m$ have been suggested at room temperature, present results conclude that the structure at room temperature is the $Fd\bar{3}m$ structure, and all Raman-active phonons have been assigned in the $Fd\bar{3}m$ structure. No remarkable difference has been found at the superconducting transition temperature, 9.6 K, and at the first-order transition temperature, 7.5 K, in the present accuracy. More accurate measurements are necessary to detect the anomaly, e.g., measurements below 25 cm^{-1} and higher resolution measurements.

As expected from the anomalously large atomic displacement parameter of potassium, the $T_{2g}(1)$ mode, which is a vibration of potassium, shows large anharmonicity; that is, the energy decreases by 8.9 cm^{-1} from room temperature to 4 K. This change in energy is very large in comparison with other cage compounds.[10–13] In addition, the $T_{2g}(2)$ and E_g modes, which are vibrations of oxygen also show the large change as observed in the $T_{2g}(1)$ mode. This result indicates that vibrations of oxygen also have a large amplitude and are highly anharmonic. To understand the oxygen case, we propose the extra contribution of other low-energy phonons and point out the E_u mode as the counterphonon of E_g.

Linewidths of phonons are proportional to temperature. The temperature variations are governed by the scattering process caused by low-energy phonons and electronic excitations. The similar gradients for the observed four phonons show the similar scattering of phonons at high temperature.

The magnitude of electron-lattice interactions is estimated from the value at 4 K. The $T_{2g}(4)$ mode, which modifies mainly bonds between osmium and oxygen, is affected by large electron-lattice interactions. This is consistent with electronic states on the Fermi surfaces that are constructed by d electrons of osmium and p electrons of oxygen. The mode with the next strong electron-lattice interactions is the E_g mode. This deduces that the oxygen E_u mode also has intensive electron-lattice interactions.

The oxygen E_u mode is the soft mode for the structural phase transition at 200 K in the superconducting pyrochlore compound of $Cd_2Re_2O_6$. The present result shows that in the superconducting β-pyrochlore compound, KOs_2O_6, the E_u mode has a low energy and strong electron-lattice interactions. Therefore, in addition to potassium vibrations, which have attracted much interest in KOs_2O_6, the E_u mode of oxygen is important for the superconductivity and/or the structural transition in β-pyrochlore superconducting oxides.

ACKNOWLEDGMENTS

This work was supported by a Grant-in-Aid for Scientific Research Priority Area "Skutterudite" (Grant No. 15072205) of Ministry of Education, Sports, Culture, Science and Technology. The experiments have been supported by N-BARD and IAMR of Hiroshima University. Figure 2 was drawn, thanks to VICS-II developed by Momma and Izawa.

---

*hase@hiroshima-u.ac.jp

[1] J. Kuneš, T. Jeong, and W. E. Pickett, Phys. Rev. B **70**, 174510 (2004).

[2] Z. Hiroi, J. Yamaura, S. Yonezawa, and H. Harima, Physica C **460-462**, 20 (2007).

[3] Z. Hiroi, S. Yonezawa, Y. Nagao, and J. Yamaura, Phys. Rev. B **76**, 014523 (2007).

[4] K. Hattori, Y. Hirayama, and K. Miyake, J. Phys. Soc. Jpn. **74**, 3306 (2005).

[5] J. Yamaura, S. Yonezawa, Y. Muraoka, and Z. Hiroi, J. Solid State Chem. **179**, 336 (2006).

[6] G. Schuck, S. M. Kazakov, K. Rogacki, N. D. Zhigadlo, and J. Karpinski, Phys. Rev. B **73**, 144506 (2006).

[7] Z. Hiroi, S. Yonezawa, T. Muramatsu, J. Yamaura, and Y. Muraoka, J. Phys. Soc. Jpn. **74**, 1255 (2005).

[8] Z. Hiroi, S. Yonezawa, J. Yamaura, T. Muramatsu, Y. Matsushita, and Y. Muraoka, J. Phys. Soc. Jpn. **74**, 3400 (2005).

[9] M. Yoshida, K. Arai, R. Kaido, M. Takigawa, S. Yonezawa, Y. Muraoka, and Z. Hiroi, Phys. Rev. Lett. **98**, 197002 (2007).

[10] Y. Takasu, T. Hasegawa, N. Ogita, M. Udagawa, M. A. Avila, K. Suekuni, I. Ishii, T. Suzuki, and T. Takabatake, Phys. Rev. B **74**, 174303 (2006).

[11] Y. Takasu, T. Hasegawa, N. Ogita, M. Udagawa, M. A. Avila, and T. Takabatake, J. Magn. Magn. Mater. **310**, 954 (2007).

[12] T. Hasegawa, Y. Takasu, T. Kondou, N. Ogita, M. Udagawa, T. Yamaguchi, T. Watanabe, Y. Nemoto, and T. Goto, J. Magn. Magn. Mater. **310**, 984 (2007).

[13] K. Iwasa, M. Kohgi, H. Sugawara, and H. Sato, Physica B **378-380**, 194 (2006).

[14] S. Yonezawa, Y. Muraoka, Y. Matsushita, and Z. Hiroi, J. Phys.: Condens. Matter **16**, L9 (2004).

[15] S. Yonezawa, Y. Muraoka, Y. Matsushita, and Z. Hiroi, J. Phys. Soc. Jpn. **73**, 819 (2004).

[16] S. Yonezawa, Y. Muraoka, and Z. Hiroi, J. Phys. Soc. Jpn. **73**, 1655 (2004).

[17] M. Brühwiler, S. M. Kazakov, N. D. Zhigadlo, J. Karpinski, and B. Batlogg, Phys. Rev. B **70**, 020503(R) (2004).

[18] M. Hanawa, Y. Muraoka, T. Tayama, T. Sakakibara, J. Yamaura, and Z. Hiroi, Phys. Rev. Lett. **87**, 187001 (2001).

[19] H. Sakai, K. Yoshimura, H. Ohno, H. Kato, S. Kambe, R. E. Walstedt, T. D. Matsuda, Y. Haga, and Y. Onuki, J. Phys.: Condens. Matter **13**, L785 (2001).

[20] R. Jin, J. He, S. McCall, C. S. Alexander, F. Drymiotis, and D. Mandrus, Phys. Rev. B **64**, 180503(R) (2001).

[21] J. Kuneš and W. E. Pickett, Phys. Status Solidi A **203**, 2962 (2006).

[22] J. Kuneš and W. E. Pickett, Phys. Rev. B **74**, 094302 (2006).

[23] J. Kuneš and W. E. Pickett, Physica B **378-380**, 898 (2006).

[24] Z. Hiroi, S. Yonezawa, J. Yamaura, T. Muramatsu, and Y. Muraoka, J. Phys. Soc. Jpn. **74**, 1682 (2005).

[25] J. Yamaura and Z. Hiroi (private communication).

[26] C. S. Knee, J. Holmlund, J. Andreasson, M. Käll, S. G. Eriksson, and L. Börjesson, Phys. Rev. B **71**, 214518 (2005).

[27] C. A. Kendziora, I. A. Sergienko, R. Jin, J. He, V. Keppens, B. C. Sales, and D. Mandrus, Phys. Rev. Lett. **95**, 125503 (2005).

[28] K. Sasai, K. Hirota, Y. Nagao, S. Yonezawa, and Z. Hiroi, J. Phys. Soc. Jpn. **76**, 104603 (2007).

[29] The ABINIT package is a common project of the Universite Catholique de Louvain, Coring Incorporated, and other contributors (http://www.abinit.org/).

[30] X. Gonze *et al.*, Comput. Mater. Sci. **25**, 478 (2002).

[31] I. A. Sergienko and S. H. Curnoe, J. Phys. Soc. Jpn. **72**, 1607 (2003).

[32] J. Yamaura and Z. Hiroi, J. Phys. Soc. Jpn. **71**, 2598 (2002).

[33] M. T. Weller, R. W. Hughes, J. Rooke, C. S. Knee, and J. Reading, Dalton Trans. **2004**, 3032.

[34] P. B. Allen, Phys. Rev. B **6**, 2577 (1972).

[35] R. Saniz, J. E. Medvedeva, L. H. Ye, T. Shishidou, and A. J. Freeman, Phys. Rev. B **70**, 100505(R) (2004).

[36] R. Saniz and A. J. Freeman, Phys. Rev. B **72**, 024522 (2005).

[37] P. Hohenberg and W. Kohn, Phys. Rev. **136**, B864 (1964).

[38] W. Kohn and L. J. Sham, Phys. Rev. **140**, A1133 (1965).

[39] J. P. Perdew and Y. Wang, Phys. Rev. B **45**, 13244 (1992).

[40] N. Troullier and J. L. Martins, Phys. Rev. B **43**, 1993 (1991).

[41] M. Fuchs and M. Scheffler, Comput. Phys. Commun. **119**, 67 (1999).

[42] X. Gonze, Phys. Rev. B **55**, 10337 (1997).

[43] X. Gonze and C. Lee, Phys. Rev. B **55**, 10355 (1997).

[44] H. J. Monkhorst and J. D. Pack, Phys. Rev. B **13**, 5188 (1976).